Resolution of Near-Field Beamforming and Its Impact on NOMA

Zhiguo Ding, *Fellow, IEEE*

***Abstract*—The resolution of near-field beamforming is an important metric to measure how effectively users with different locations can be located. This letter identifies the condition under which the resolution of near-field beamforming is not perfect. This imperfect resolution means that one user's near-field beam can be still useful to other users, which motivates the application of non-orthogonal multiple access (NOMA). Both the analytical and simulation results are developed to demonstrate that those near-field beams preconfigured for legacy users can indeed be used to effectively serve additional NOMA users, which improves the overall connectivity and system throughput.**

***Index Terms*—Near-field communication, non-orthogonal multiple access (NOMA), resolution of near-field beamforming.**

I. Introduction

Near-field beamforming has recently received a lot of attention, due to the use of high carrier frequency bands, such as millimeter-wave (mmWave) and Terahertz (THz) bands, where the use of a massive number of antennas becomes possible and hence the Rayleigh distance becomes significantly large [1], [2]. One exciting feature of near-field beamforming is that users can be separated precisely by their locations, as explained by the following downlink multi-input single-output (MISO) example. For conventional far-field beamforming, the simplified beam-steering vector is used to model a user's channel vector, and hence two users with identical angels of departure but different distances from the base station share the same beam-steering vector, which makes it difficult for the base station to distinguish the users [3]. On the contrary, near-field beamforming can ensure that the two users can be distinguished because of the use of the sophisticated spherical-wave propagation model [4], [5]. This existing feature has led to the recent studies for resource allocation in near-field communication networks, and also the design of location based multiple access (LDMA) [6], [7].

The aim of this letter is to provide a detailed study of the feasibility of near-field beamforming to locate randomly located users. To facilitate the performance analysis, we first define the resolution of near-field beamforming in this letter, which is the cross-correlation of the users' spherical-wave channel vectors. The existing literature shows that the resolution of near-field beamforming becomes perfect, if the number of the antennas at the base station becomes infinity. In this letter, it shown that, unless the users are clustered very close to the base station, the resolution of near-field beamforming is not perfect. In particular, analytical results are developed to show that for the users which have identical angles of departure, the correlation of their channel vectors becomes almost one, if their distances to the base station are proportional to the Rayleigh distance, regardless the choices of the number of antennas. In other words, one user's near-field beam can be still useful to other users, which motivates the second contribution of this paper which is to investigate the feasibility of applying non-orthogonal multiple access (NOMA) in near-field networks [8]. Both the analytical and simulation results are developed to demonstrate that those near-field beams preconfigured for legacy users can be used to effectively serve additional NOMA users, which improves the overall connectivity and system throughput.

Z. Ding is with Department of Electrical Engineering and Computer Science, Khalifa University, Abu Dhabi, and also with Department of Electrical and Electronic Engineering, University of Manchester, Manchester, UK.

II. System Model

Consider a downlink network with M legacy users, denoted by $\mathrm{U}_m^{\mathrm{L}}$, $m \in \{0, \cdots, M\}$, where each user is equipped with a single antenna, and the base station uses a uniform linear array (ULA) with N elements. Each user receives the following observation:

$$y_m^{\mathrm{L}} = \mathbf{h}_m^H \sum_{i=1}^{M} \mathbf{p}_i x_i + n_m^{\mathrm{L}}, \tag{1}$$

where $\mathrm{U}_m^{\mathrm{L}}$'s channel vector is denoted by $\mathbf{h}_m$ and based on the spherical-wave propagation model because the legacy users' distances to the base station are assumed to be smaller than the Rayleigh distance, denoted by d_{Ray} [2], [5], [9], i.e., $\mathbf{h}_m = \sqrt{N\gamma_{\boldsymbol{\psi}_m^{\mathrm{L}}}}\mathbf{b}\left(\boldsymbol{\psi}_m^{\mathrm{L}}\right)$, $\boldsymbol{\psi}_m^{\mathrm{L}}$ denotes the m-th legacy user's location based on the Cartesian coornidate,

$$\mathbf{b}\left(\boldsymbol{\psi}\right) = \frac{1}{\sqrt{N}}\left[e^{-j\frac{2\pi}{\lambda}|\boldsymbol{\psi}-\boldsymbol{\psi}_1|} \quad \cdots \quad e^{-j\frac{2\pi}{\lambda}|\boldsymbol{\psi}-\boldsymbol{\psi}_N|}\right]^T, \tag{2}$$

$\boldsymbol{\psi}_n$ denotes the location of the n-th element of ULA, $\gamma_{\boldsymbol{\psi}_m^{\mathrm{L}}} = \frac{c^2}{16\pi^2 f_c^2 |\boldsymbol{\psi}_m^{\mathrm{L}} - \boldsymbol{\psi}_0|^2}$, c, and f_c denote the free-space path loss, the speed of light, and the carrier frequency, respectively, n_m^{L} denotes the additive Gaussian noise with power P_N, $\mathbf{p}_m$ denotes the beamforming vector, and x_m denotes the signal sent on $\mathbf{p}_m$. The legacy users and the NOMA users' locations based on the polar coordinates are denoted by $(r_m^{\mathrm{L}}, \theta_m^{\mathrm{L}})$, and $(r_k^{\mathrm{N}}, \theta_k^{\mathrm{N}})$, respectively.

As in [8], $\mathbf{p}_m$ is assumed to be preconfigured according to the legacy users' channel vectors, and the aim of the paper is to investigate the feasibility to serve additional NOMA users by using the preconfigured vectors. As commonly used in the massive MIMO literature, the maximal ratio combining type of precoding is used, i.e., $\mathbf{p}_m = \mathbf{b}\left(\boldsymbol{\psi}_m^{\mathrm{L}}\right)$, which means that $\mathbf{p}_m^H \mathbf{p}_m = 1$, and $|\mathbf{p}_m^H \mathbf{h}_m|^2 = N\gamma_{\boldsymbol{\psi}_m^{\mathrm{L}}}$.

Consider that there are K NOMA users, denoted by $\mathrm{U}_k^{\mathrm{N}}$, $k \in \{1, \cdots, K\}$, and $\mathrm{U}_k^{\mathrm{N}}$ receives the following observation:

$$y_k^{\mathrm{N}} = \mathbf{g}_k^H \sum_{i=1}^{K} \mathbf{p}_i x_i + n_k^{\mathrm{N}}, \tag{3}$$

where $\mathbf{g}_k$ and n_k^{N} are defined similar to $\mathbf{h}_m$ and n_k^{L}, respectively. Assume that $\mathrm{U}_k^{\mathrm{N}}$ is scheduled on beam $\mathbf{p}_m$, the base station sends $x_m = \sqrt{P_S \alpha_m^{\mathrm{L}}} s_m^{\mathrm{L}} + \sqrt{P_S \alpha_m^{\mathrm{N}}} s_k^{\mathrm{N}}$, where P_S denotes the transmit power budget for each user s_m^{L} and s_k^{N} denote the signals to $\mathrm{U}_m^{\mathrm{L}}$ and $\mathrm{U}_k^{\mathrm{N}}$, respectively, α_m^{L} and α_m^{N} denote the NOMA power allocation coefficients, and $\alpha_m^{\mathrm{N}} + \alpha_m^{\mathrm{L}} = 1$. To avoid disruption to the legacy users' quality of experience, the NOMA users' signals will be decoded first on each beam, which means that the data rate of the NOMA user, $\mathrm{U}_k^{\mathrm{N}}$, on beam $\mathbf{p}_m$ is given by $R_k^{\mathrm{N}} = \log\left(1 + \frac{P_S N \gamma_{\boldsymbol{\psi}_k^{\mathrm{N}}} \alpha_m^{\mathrm{N}} |\mathbf{b}(\boldsymbol{\psi}_m^{\mathrm{L}})^H \mathbf{b}(\boldsymbol{\psi}_k^{\mathrm{N}})|^2}{P_S N \gamma_{\boldsymbol{\psi}_k^{\mathrm{N}}} \alpha_m^{\mathrm{L}} |\mathbf{b}(\boldsymbol{\psi}_m^{\mathrm{L}})^H \mathbf{b}(\boldsymbol{\psi}_k^{\mathrm{N}})|^2 + + P_N}\right)$, where $I_k^{\mathrm{N}} = \sum_{\substack{i=1 \\ i \neq m}}^{M} P_S N \gamma_{\boldsymbol{\psi}_k^{\mathrm{N}}} |\mathbf{b}\left(\boldsymbol{\psi}_i^{\mathrm{L}}\right)^H \mathbf{b}\left(\boldsymbol{\psi}_k^{\mathrm{N}}\right)|^2$. Because the legacy user has a strong channel gain, it first decodes its partner's signal with the following data rate: $\tilde{R}_m^{\mathrm{L}} = \log\left(1 + \frac{P_S N \gamma_{\boldsymbol{\psi}_m^{\mathrm{L}}} \alpha_m^{\mathrm{N}} |\mathbf{b}(\boldsymbol{\psi}_m^{\mathrm{L}})^H \mathbf{b}(\boldsymbol{\psi}_m^{\mathrm{L}})|^2}{P_S N \gamma_{\boldsymbol{\psi}_m^{\mathrm{L}}} \alpha_m^{\mathrm{L}} |\mathbf{b}(\boldsymbol{\psi}_m^{\mathrm{L}})^H \mathbf{b}(\boldsymbol{\psi}_m^{\mathrm{L}})|^2 + I_m^{\mathrm{L}} + P_N}\right)$, where I_m^{L} is defined similarly to I_k^{N}. If the first stage of SIC is successful, the legacy user can decodes its own message with the following data rate: $R_m^{\mathrm{L}} = \log\left(1 + \frac{P_S N \gamma_{\boldsymbol{\psi}_m^{\mathrm{L}}} \alpha_m^{\mathrm{L}} |\mathbf{b}(\boldsymbol{\psi}_m^{\mathrm{L}})^H \mathbf{b}(\boldsymbol{\psi}_m^{\mathrm{L}})|^2}{\sum_{\substack{i=1 \\ i \neq m}}^{M} P_S N \gamma_{\boldsymbol{\psi}_m^{\mathrm{L}}} |\mathbf{b}(\boldsymbol{\psi}_i^{\mathrm{L}})^H \mathbf{b}(\boldsymbol{\psi}_m^{\mathrm{L}})|^2 + P_N}\right)$.

One of the new features in the near-field literature is that $|\mathbf{b}\left(\boldsymbol{\psi}_m^{\mathrm{L}}\right)^H \mathbf{b}\left(\boldsymbol{\psi}_k^{\mathrm{N}}\right)|^2 \to 0$, for $N \to \infty$.

As can be seen from the expressions of R_k^{N}, $\tilde{R}_m^{\mathrm{L}}$, and R_m^{L}, these data rates

III. Resolution of Near-Field Beamforming

The resolution of near-field beamforming can be defined as $\Delta \triangleq \left|\mathbf{b}\left(\boldsymbol{\psi}_1\right)^H \mathbf{b}\left(\boldsymbol{\psi}_2\right)\right|^2$, for any $\boldsymbol{\psi}_1 \neq \boldsymbol{\psi}_2$, which is to be evaluated in this section. Define (r_i, θ_i) as the polar coordinates corresponding to $\boldsymbol{\psi}_i$, $i \in \{1, 2\}$.

In the distance domain, the resolution of near-field beamforming is shown to be asymptotically perfect, i.e., $\Delta \triangleq \left|\mathbf{b}\left(\boldsymbol{\psi}_1\right)^H \mathbf{b}\left(\boldsymbol{\psi}_2\right)\right|^2 \to 0$, for $N \to \infty$, if $\theta_1 = \theta_2$ [6]. The following lemma illustrates that the resolution of near-field beamforming in the distance domain cannot be perfect, even if $N \to \infty$.

Lemma 1. *Assume that $\theta_1 = \theta_2 \triangleq \theta_0$ and $r_i = \beta_i d_{\mathrm{Ray}}$. If $\tau \triangleq (1 - \sin^2\theta_0)\left(\frac{1}{\beta_1} - \frac{1}{\beta_2}\right) \to 0$, Δ can be approximated as follows:*

$$\Delta \approx 1 - \frac{\pi^2 \tau^2 (N+1)}{5760(N-1)^3}\left(26N^2 - 38\right). \tag{4}$$

Proof. See Appendix A. □

Define $f(x) = \frac{(x+1)\left(26x^2-38\right)}{(x-1)^3}$ whose first-order derivative is given by $f'(x) = \frac{-104x^2+24x+152}{(x-1)^4}$. The largest root of $f'(x) = 0$ is 1.33, which means $f'(n) < 0$, for $n = \{2, 3, \cdots\}$. Therefore, $f(N)$ is a monotonically decreasing function of N, which leads to the following corollary.

Corollary 1. *Assume that $\theta_1 = \theta_2 \triangleq \theta_0$ and $r_m = \beta_m d_{\mathrm{Ray}}$. If $\tau \triangleq (1 - \sin^2\theta_0)\left(\frac{1}{\beta_1} - \frac{1}{\beta_2}\right) \to 0$, Δ is a monotonically increasing function of N, and with $N \to \infty$, Δ becomes a constant as follows:*

$$\Delta \to 1 - \frac{13\pi^2\tau^2}{2880}. \tag{5}$$

Remark 1: Lemma 1 and Corollary 1 indicate that the resolution of NF beamforming is not perfect in the distance domain. This features facilitates the implementation of NOMA, where a beam preconfigured to a legacy user can be still useful to those users which are located on the direction of the beam.

Remark 2: In [6], it was stated that $\Delta \to 0$ for $N \to \infty$, which is true only if one or both the users are very close to the base station, which makes $\left|\frac{1}{r_1} - \frac{1}{r_2}\right|$ large, and with large τ, the approximation in Lemma 1 becomes not applicable. Nevertheless, for many users which are not close from the base station, the resolution of near-field beamforming is limited, which motivates the implementation of NOMA in NF-SDMA networks, as shown in the following section.

IV. A Case Study for Application of NOMA

Lemma 1 and Corollary 1 indicate that a preconfigured near-field beam can be still used to admit additional users whose locations are not at the focal point of the beam. Therefore, in this section, we focus on a special case with a single legacy user, i.e., $M = 1$, where the locations of the NOMA users follow a Poisson line process. n particular, assume that the NOMA users' locations follow a one-dimensional homogeneous Poisson point process (HPPP) with density λ, and all the NOMA users are assumed to be on the segment which is between the legacy user and the cell boundary and aligned with the preconfigured beam, i.e., $\theta_1^{\mathrm{L}} = \theta_k^{\mathrm{N}}$, $k = 1, 2, \cdots$. A practical example is that the legacy user is on a street and the preconfigured beam is aligned with the street, where it is reasonable to assume that there are multiple users and devices on the street.

Furthermore, assume that the NOMA users are ordered according to their distances to the legacy user, and $\mathrm{U}_k^{\mathrm{N}}$ is the k-th closest neighbour of the legacy user, i.e., $d_1 \leq d_2 \leq \cdots$, where $d_k = \left|\boldsymbol{\psi}_k^{\mathrm{N}} - \boldsymbol{\psi}_1^{\mathrm{L}}\right|$. The cumulative distribution function (CDF) of d_k is the probability to have less than k users on a segment with the length d_k [10]:

$$F_k(r) = 1 - \sum_{i=0}^{k-1} e^{-\lambda r} \frac{\lambda^i r^i}{i!}, \tag{6}$$

which means that the probability density function (pdf) of d_k can be obtained as follows:

$$\begin{aligned} f_k(r) =& e^{-\lambda r}\left(\sum_{i=0}^{k-1} \frac{1}{i!}\lambda^{i+1} r^i - \sum_{i=0}^{k-1} \frac{1}{i!} i \lambda^i r^{i-1}\right) \\ =& e^{-\lambda r} \frac{1}{(k-1)!} \lambda^k r^{k-1}. \end{aligned} \tag{7}$$

For the considered special case with $M = 1$, the NOMA user's data rate is given by $R_k^{\mathrm{N}} =$

$\log\left(1+\frac{P_S N\gamma_{\boldsymbol{\psi}_k^{\mathrm{N}}}\alpha_m^{\mathrm{N}}|\mathbf{b}(\boldsymbol{\psi}_m^{\mathrm{L}})^H\mathbf{b}(\boldsymbol{\psi}_k^{\mathrm{N}})|^2}{P_S N\gamma_{\boldsymbol{\psi}_k^{\mathrm{N}}}\alpha_m^{\mathrm{L}}|\mathbf{b}(\boldsymbol{\psi}_m^{\mathrm{L}})^H\mathbf{b}(\boldsymbol{\psi}_k^{\mathrm{N}})|^2+P_N}\right)$, which means that the outage probability for the NOMA user $\mathrm{U}_k^{\mathrm{N}}$ is given by

$$\mathbb{P}^o=\sum_{i=0}^{k-1}\mathbb{P}(K=i)+\sum_{i=k}^{\infty}\mathbb{P}(K=i) \tag{8}$$
$$\times\,\mathbb{P}\left(\log\left(1+\frac{P_S N\gamma_{\boldsymbol{\psi}_k^{\mathrm{N}}}\alpha_m^{\mathrm{N}}|\mathbf{b}\left(\boldsymbol{\psi}_m^{\mathrm{L}}\right)^H\mathbf{b}\left(\boldsymbol{\psi}_k^{\mathrm{N}}\right)|^2}{P_S N\gamma_{\boldsymbol{\psi}_k^{\mathrm{N}}}\alpha_m^{\mathrm{L}}|\mathbf{b}\left(\boldsymbol{\psi}_m^{\mathrm{L}}\right)^H\mathbf{b}\left(\boldsymbol{\psi}_k^{\mathrm{N}}\right)|^2+P_N}\right)\le R\right),$$

where R denotes the NOMA users' target data rate, and $\mathbb{P}(K=i)$ denotes the probability of the event where there are i NOMA users on the segment.

Assume that θ_1^{L} is large and τ is small, and the use of Lemma 1 can simplify the expression of the outage probability as follows:

$$\mathbb{P}^o\approx\sum_{i=0}^{k-1}\mathbb{P}(K=i)+\sum_{i=k}^{\infty}\mathbb{P}(K=i)\times \tag{9}$$
$$\mathbb{P}\left(\frac{\frac{\eta_2}{\left(r_1^{\mathrm{L}}+r\right)^2}\alpha_m^{\mathrm{N}}\left(1-\eta_1\left(\frac{1}{r_1^{\mathrm{L}}}-\frac{1}{r_1^{\mathrm{L}}+r}\right)^2\right)}{\frac{\eta_2}{\left(r_1^{\mathrm{L}}+r\right)^2}\alpha_m^{\mathrm{L}}\left(1-\eta_1\left(\frac{1}{r_1^{\mathrm{L}}}-\frac{1}{r_1^{\mathrm{L}}+r}\right)^2\right)+P_N}\le\epsilon_1\right)$$
$$=\sum_{i=0}^{k-1}\mathbb{P}(K=i)+\sum_{i=k}^{\infty}\mathbb{P}(K=i)$$
$$\times\,\mathbb{P}\left(\frac{\eta_2}{\left(r_1^{\mathrm{L}}+r\right)^2}\left(1-\eta_1\left(\frac{1}{r_1^{\mathrm{L}}}-\frac{1}{r_1^{\mathrm{L}}+r}\right)^2\right)\le\epsilon_2\right),$$

where $\epsilon_1=2^R-1$, $\epsilon_2=\frac{P_N\epsilon_1}{\alpha_m^{\mathrm{N}}-\alpha_m^{\mathrm{L}}\epsilon_1}$, $\eta_1=\frac{\pi^2(N+1)\left(26N^2-38\right)}{5760(N-1)^3}(1-\sin^2\theta_0)^2d_{\mathrm{Ray}}^2$, and $\eta_2=\frac{P_S N c^2}{16\pi^2 f_c^2}$.

Denote the four roots of the following equation by $z_1\ge\cdots\ge z_4$:

$$-\eta_1x^4+\frac{2\eta_1}{r_1^{\mathrm{L}}}x^3+\left(1-\frac{\eta_1}{\left(r_1^{\mathrm{L}}\right)^2}\right)x^2-\frac{\epsilon_2}{\eta_2}=0. \tag{10}$$

We note that the roots are constants and not related to the users' random locations. For the considered geometric scenario with large d_{Ray}, we note that there are two positive roots, i.e., $z_1\ge z_2>0$. Therefore, the outage probability can be calculated as follows:

$$\mathbb{P}^o=\sum_{i=0}^{k-1}\mathbb{P}(K=i)+\sum_{i=k}^{\infty}\mathbb{P}(K=i) \tag{11}$$
$$\times\left[\mathbb{P}\left(R_D-r_1^{\mathrm{L}}\ge r\ge\max\left\{0,\frac{1}{z_2}-r_1^{\mathrm{L}}\right\}\right)\right.$$
$$\left.+\mathbb{P}\left(r\le\min\left\{\max\left\{0,\frac{1}{z_1}-r_1^{\mathrm{L}}\right\},R_D-r_1^{\mathrm{L}}\right\}\right)\right]$$

By using the pdf of d_k, the outage probability is given by

$$\mathbb{P}^o\approx\sum_{i=0}^{k-1}\mathbb{P}(K=i)+\sum_{i=k}^{\infty}\mathbb{P}(K=i)\frac{1}{(k-1)!} \tag{12}$$
$$\times\left(\gamma\left(k,\lambda\left(R_D-r_1^{\mathrm{L}}\right)\right)-\gamma\left(k,\lambda\max\left\{0,\frac{1}{z_2}-r_1^{\mathrm{L}}\right\}\right)\right.$$
$$\left.+\,\gamma\left(k,\lambda\min\left\{\max\left\{0,\frac{1}{z_1}-r_1^{\mathrm{L}}\right\},R_D-r_1^{\mathrm{L}}\right\}\right)\right),$$

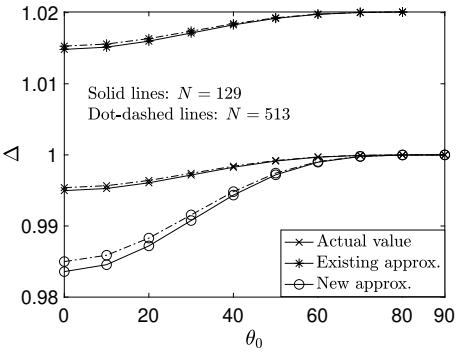

Fig. 1. Impact of θ_0 on the resolution of near-field beamforming, Δ, where $\theta_i=\theta_0$, $r_i=\beta_i d_{\mathrm{Ray}}$, $i\in\{1,2\}$, $\beta_1=0.5$ and $\beta_2=0.2+\beta_1$.

where [11, equation 3.381] is used.

With some algebraic manipulations, the following corollary can be obtained for the outage probability.

Corollary 2. *By assuming that the NOMA users follows the one-dimensional HPPP and $\tau\to 0$, the outage probability for the k-th nearest neighbour to the legacy user is given by*

$$\mathbb{P}^o\approx\sum_{i=0}^{k-1}e^{-\lambda(R_D-r_1^{\mathrm{L}})}\frac{\lambda^i(R_D-r_1^{\mathrm{L}})^i}{i!} \tag{13}$$
$$+\sum_{i=k}^{\infty}e^{-\lambda(R_D-r_1^{\mathrm{L}})}\frac{\lambda^i(R_D-r_1^{\mathrm{L}})^i}{i!}\frac{1}{(k-1)!}$$
$$\times\left(\gamma\left(k,\lambda\left(R_D-r_1^{\mathrm{L}}\right)\right)-\gamma\left(k,\lambda\max\left\{0,\frac{1}{z_2}-r_1^{\mathrm{L}}\right\}\right)\right.$$
$$\left.+\,\gamma\left(k,\lambda\min\left\{\max\left\{0,\frac{1}{z_1}-r_1^{\mathrm{L}}\right\},R_D-r_1^{\mathrm{L}}\right\}\right)\right).$$

V. Numerical Studies

In this section, computer simulation results are presented to demonstrate the resolution of near-field beamforming, and its impact on the implementation of NOMA. For all the carried out simulations, the carrier frequency of 28 GHz is used, the noise power is -80 dBm, and the antenna spacing for the ULA is set to be half of the wavelength.

In Figs. 1 and 2, the impact of θ_0 on the resolution of near-field beamforming, $\Delta\triangleq\left|\mathbf{b}\left(\boldsymbol{\psi}_1\right)^H\mathbf{b}\left(\boldsymbol{\psi}_2\right)\right|^2$, for any $\boldsymbol{\psi}_1\neq\boldsymbol{\psi}_2$, is investigated. In Fig. 1, the two users' distances to the base station are proportional to the Rayleigh distance, i.e., $r_i=\beta_i d_{\mathrm{Ray}}$, $i\in\{1,2\}$. In this case, Fig. 1 shows that the resolution of near-field beamforming is poor, particular, if θ_0 is large. In addition, the figure also demonstrates that the new approximation results developed in this paper are more accurate that the existing ones, particularly for large θ_0. An interesting observation from Fig. 1 is that the resolution of near-field beamforming gets slightly poorer if more antennas are used. In Fig. 2, the users are deployed close to the base station, where their distances to the base station are no longer proportional to the Rayleigh distance. In this case, Fig. 2 demonstrates that the resolution of near-field beamforming becomes accurate, particularly if the users are very close to the base station, or the number of antennas becomes very large.

In Figs. 1 and 2 show that the resolution of near-field beamforming is poor, unless the users are clustered close to

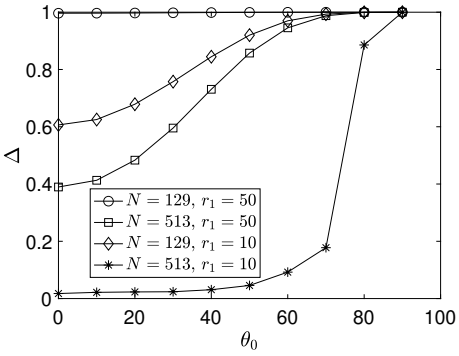

Fig. 2. Impact of θ_0 on the resolution of near-field beamforming, Δ, where $\theta_i = \theta_0$, $i \in \{1, 2\}$, and $r_1 - r_2 = 20$.

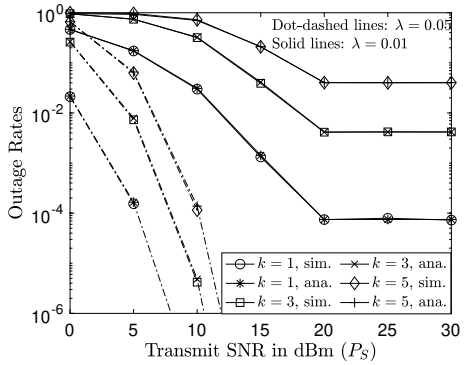

(a) $N = 129$, $\theta_0 = 45^0$

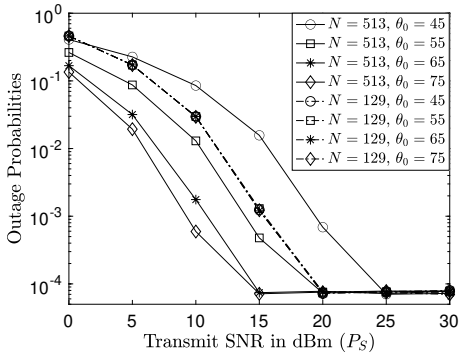

(b) $\lambda = 0.01$ and $k = 1$

Fig. 3. Outage probability of the scheduled NOMA user by using the Poisson line process. $M = 1$, $r_1^{\mathrm{L}} = 50$, $R_D = 1000$, $R = 0.5$ BPCU, $\alpha_m^{\mathrm{N}} = \frac{4}{5}$ and $\alpha_m^{\mathrm{L}} = \frac{1}{5}$.

the base station, which demonstrates the feasibility of using NOMA, as the users are most likely randomly deployed in the network. In Fig. 3, the NOMA users are assumed to be randomly deployed on the segment which is on the direction of $\mathrm{U}_1^{\mathrm{L}}$'s channel vector and between $\mathrm{U}_1^{\mathrm{L}}$ and the boundary of the cell, where there is a single legacy user, $M = 1$, the radius of the cell is denoted by D_R and the k-th NOMA closest to the base station is scheduled. Fig. 4(a) shows that the scheduled NOMA user's outage probability can be reduced significantly either by increasing the user intensity, λ, or by reducing the distance between the scheduled user and the base station, i.e., reduce k. Fig. 4(b) shows that the user's outage probability can be further reduced by increasing θ_0 for the case of $N = 513$, whereas the impact of θ_0 on the outage probability is insignificant. Fig. 4(a) also demonstrates the accuracy of the developed outage probability expression shown

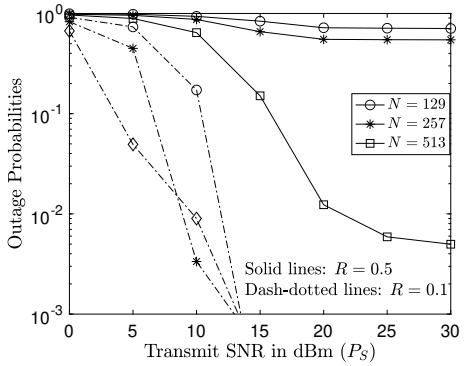

(a) Outage Probabilites

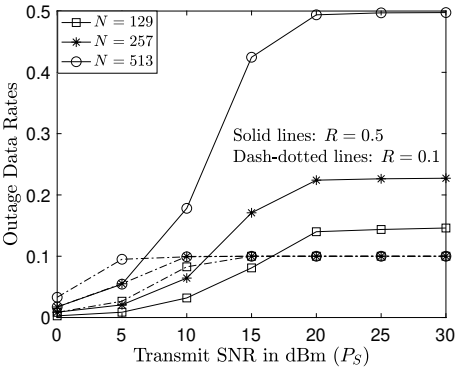

(b) Outage Rates

Fig. 4. Outage probability of the scheduled NOMA user by using the Poisson cluster process. $M = 36$, $\lambda = 0.05$, $r^{\mathrm{L}} = 50$, $R_D = 1000$, $R_c = 10$, $\alpha_m^{\mathrm{N}} = \frac{4}{5}$ and $\alpha_m^{\mathrm{L}} = \frac{1}{5}$.

in Corollary 2.

A natural extension of Fig. 3 is to consider that the locations of the NOMA users follow a Poisson point process in the whole cell. However, for a cell with radius being 1000 m, the averaged number of the NOMA users is around 3000, which makes it challenging to carry out Monte Carlo simulations. Therefore, in Fig. 4, a Poisson cluster process is adapted, where the NOMA users are clustered within a disc with radius R_c, the center of the disc is uniformly located within the cell, and the NOMA user with the best channel gain is scheduled. On the other hand, the legacy users are equally spaced and located on a semicircle with radius 50 m. As can be seen from the figure, the scheduled NOMA user can be served with a reasonable outage probability, which means that the near-field beams for the legacy users can be used to efficiently serve NOMA users randomly located within the cell. We note that increasing the target data rate R can increase the achievable outage rate, but decreases the outage probability. Furthermore, it is important to point out that the use of more antennas can effectively increase the outage data rate of the NOMA user, an important property given the fact that massive MIMO is envisioned to be employed in future wireless networks.

VI. Conclusions

In this letter, the condition under which the resolution of near-field beamforming is not perfect has been identified. This imperfect resolution means that one user's near-field beam can be still useful to other users, which motivates the case study for the application of NOMA. Both the analytical and simulation

results have been developed to demonstrate that those near-field beams preconfigured for legacy users can indeed be used to effectively serve additional NOMA users, which improves the overall connectivity and system throughput. The analytical results obtained in this letter are also consistent to the findings previously reported in [8].

Appendix A
Proof for Lemma 1

By using the spherical-wave propagation model, the resolution of near-field beamforming, which is also the cross-correlation of the users' channel vector, i.e., $\Delta \triangleq \left|\mathbf{b}\left(\boldsymbol{\psi}_1\right)^H \mathbf{b}\left(\boldsymbol{\psi}_2\right)\right|^2$, can be expressed as follows:

$$\Delta = \left|\sum_{n=1}^{N} e^{-j\frac{2\pi}{\lambda}\left(|\boldsymbol{\psi}_1-\boldsymbol{\psi}_n|-|\boldsymbol{\psi}_2-\boldsymbol{\psi}_n|\right)}\right|^2. \tag{14}$$

Recall that each distance can be expressed as $|\boldsymbol{\psi}_m - \boldsymbol{\psi}_n| = r_m\sqrt{1+\frac{d_n^2-2r_m d_n\sin\theta_m}{r_m^2}}$, for $m \in \{1,2\}$, where $d_n = d\left(n-1-\frac{N-1}{2}\right)$ and d denotes the antenna spacing of the ULA. Note that r_m is assumed to be proportional to d_{Ray}, and hence $\frac{d_n^2-2r_m d_n\sin\theta_m}{r_m^2} \to 0$, which leads to the following approximation:

$$|\boldsymbol{\psi}_m - \boldsymbol{\psi}_n| \approx r_m\left(1-\frac{d_n\sin\theta_m}{r_m}+\frac{d_n^2(1-\sin^2\theta_m)}{2r_m^2}\right), \tag{15}$$

which is based on the following approximation: $(1+x)^{\frac{1}{2}} \approx 1+\frac{1}{2}x-\frac{1}{8}x^2$ for $x \to 0$.

By applying the approximation in (15), Δ can be simplified as follows:

$$\begin{aligned}\Delta &\approx \left|\sum_{n=1}^{N} e^{-j\frac{2\pi}{\lambda}\left(\frac{d_n^2(1-\sin^2\theta_0)}{2r_1}-\frac{d_n^2(1-\sin^2\theta_0)}{2r_2}\right)}\right|^2 \\ &= \left|\sum_{k=-\frac{N-1}{2}}^{\frac{N-1}{2}} e^{j\pi k^2 d^2\frac{1}{\lambda}(1-\sin^2\theta_0)\left(\frac{1}{r_1}-\frac{1}{r_2}\right)}\right|^2.\end{aligned} \tag{16}$$

In the literature, the above sum was shown to go to zero if $N \to \infty$ [6], which is not accurate if the users' distances to the base station are proportional to the Rayleigh distance, as shown in the following.

In particular, assume that $r_1 = \beta_1 d_{\text{Ray}}$ and $r_2 = \beta_2 d_{\text{Ray}}$, where $d_{\text{Ray}} = \frac{2d^2(N-1)^2}{\lambda}$. By substituting the expressions of r_1 and r_2 to (16), Δ can be expressed as follows:

$$\Delta \approx \left|\sum_{k=-\frac{N-1}{2}}^{\frac{N-1}{2}} e^{j\pi k^2\frac{1}{2(N-1)^2}(1-\sin^2\theta_0)\left(\frac{1}{\beta_1}-\frac{1}{\beta_2}\right)}\right|^2. \tag{17}$$

By using the expression of τ, Δ can be expressed as follows:

$$\Delta = \left|\sum_{k=-\frac{N-1}{2}}^{\frac{N-1}{2}} \cos\left(\tilde{\theta}_k\right)+j\sin\left(\frac{\pi k^2}{2(N-1)^2}\tau\right)\right|^2, \tag{18}$$

where $\tilde{\theta}_k = \frac{\pi k^2}{2(N-1)^2}\tau$ If $\tau \to 0$, Δ can be further approximated as follows:

$$\begin{aligned}\Delta &\overset{(a)}{\approx} \left|N-\sum_{k=-\frac{N-1}{2}}^{\frac{N-1}{2}}\tilde{\theta}_k^2+j\sum_{k=-\frac{N-1}{2}}^{\frac{N-1}{2}}\tilde{\theta}_k\right|^2 \\ &\approx 1-2N\sum_{k=-\frac{N-1}{2}}^{\frac{N-1}{2}}\tilde{\theta}_k^2+\left(\sum_{k=-\frac{N-1}{2}}^{\frac{N-1}{2}}\tilde{\theta}_k\right)^2 \\ &= 1-\frac{\pi^2\tau^2}{N(N-1)^4}\sum_{k=1}^{\frac{N-1}{2}}k^4+\frac{\pi^2\tau^2}{N^2(N-1)^4}\left(\sum_{k=1}^{\frac{N-1}{2}}k^2\right)^2,\end{aligned} \tag{19}$$

where step (a) is obtained by using the following approximation: $\cos(x) \approx 1-x^2$ and $\sin(x) = x$ for $x \to 0$.

By using the two following finite sums, $\sum_{k=1}^{n}k^4 = \frac{n(n+1)(2n+1)(3n^2+3n-1)}{30}$ and $\sum_{k=1}^{n}k^2 = \frac{n(n+1)(2n+1)}{6}$, Δ can be further approximated as follows:

$$\begin{aligned}\Delta \approx& 1-\frac{\pi^2\tau^2}{N(N-1)^4}\frac{N(N-1)(N+1)(3N^2-4)}{480} \\ &+\frac{\pi^2\tau^2}{N^2(N-1)^4}\left(\frac{N(N-1)(N+1)}{24}\right)^2.\end{aligned} \tag{20}$$

With some straightforward algebraic manipulations, the approximated expression shown in the lemma can be obtained, and the proof is complete.

References

[1] R. W. Heath, N. Gonzalez-Prelcic, S. Rangan, W. Roh, and A. M. Sayeed, "An overview of signal processing techniques for millimeter wave MIMO systems," *IEEE J. Sel. Topics Signal Process.*, vol. 10, no. 3, pp. 436–453, Apr. 2016.

[2] J. Zhu, Z. Wan, L. Dai, M. Debbah, and H. V. Poor, "Electromagnetic information theory: Fundamentals, modeling, applications, and open problems," Available on-line at arXiv:2209.09562, 2022.

[3] Y. Zou, W. Rave, and G. Fettweis, "Analog beamsteering for flexible hybrid beamforming design in mmWave communications," in *Proc. EuCNC*, Athens, Greece, Jun. 2016.

[4] E. Björnson, L. Sanguinetti, H. Wymeersch, J. Hoydis, and T. L. Marzetta, "Massive MIMO is a reality - what is next?: Five promising research directions for antenna arrays," *Digital Signal Processing*, vol. 94, pp. 3–20, Oct. 2019.

[5] H. Zhang, N. Shlezinger, F. Guidi, D. Dardari, M. F. Imani, and Y. C. Eldar, "Beam focusing for near-field multiuser MIMO communications," *IEEE Trans. Wireless Commun.*, vol. 21, no. 9, pp. 7476–7490, Sept. 2022.

[6] Z. Wu and L. Dai, "Multiple access for near-field communications: SDMA or LDMA?" Available on-line at arXiv:2208.06349, 2022.

[7] Y. Liu, Z. Wang, J. Xu, C. Ouyang, X. Mu, and R. Schober, "Near-field communications: A tutorial review," Available on-line at arXiv:2305.17751, 2023.

[8] Z. Ding, R. Schober, and H. V. Poor, "NOMA-based coexistence of near-field and far-field massive MIMO communications," *IEEE Wireless Communications Letters*, pp. 1–1, 2023.

[9] X. Zhang, H. Zhang, and Y. C. Eldar, "Near-field sparse channel representation and estimation in 6G wireless communications," Available on-line at arXiv:2212.13527, 2022.

[10] M. Haenggi, *Stochastic Geometry for Wireless Networks*. Cambridge University Press, Cambridge, UK, 2012.

[11] I. S. Gradshteyn and I. M. Ryzhik, *Table of Integrals, Series and Products*, 6th ed. New York: Academic Press, 2000.